Influence of boric acid on the hydration of magnesium phosphate cement at an early age

H. Lahalle, C. Cauditcoumes, D. Lambertin, C. Cannes, S. Delpech, S. Gauffinet

Influence of boric acid on the hydration of magnesium phosphate cement at an early age

LAHALLE Hugo[1], CAU DIT COUMES Céline[1*], LAMBERTIN David[1], CANNES Céline[2], DELPECH Sylvie[2], GAUFFINET Sandrine[3]

1. CEA, DEN, DTCD, SPDE, F-30207 Bagnols-sur-Cèze cedex, France

2. Institut de Physique Nucléaire, CNRS, Univ. Paris-Sud 11, 91406 Orsay Cedex, France

3. UMR6303 Laboratoire Interdisciplinaire Carnot de Bourgogne, Université de Bourgogne Dijon, Faculté des Sciences Mirande, 9 Avenue Alain Savary, BP 47870, 21078 Dijon cedex, France

Abstract

Magnesium phosphate cements (MPCs) are receiving increasing attention because of their outstanding properties of fast setting and hardening, good volume stability and excellent bonding to old concrete structures. Their main area of application is thus rapid repair works, but they may also offer prospects for the stabilization / solidification of deleterious waste.

The main constituents of MPCs are magnesium oxide (calcined, or "hardburnt", magnesia) and a water-soluble acid phosphate, which is most often diammonium hydrogen phosphate $(NH_4)_2HPO_4$. To avoid the release of noxious gaseous ammonia during the hardening process, potassium dihydrogen phosphate (KH_2PO_4) is used. The main precipitated hydrate is then K-struvite ($MgKPO_4.6H_2O$). This paper aims at giving new insight into the processes involved in its formation. Since the reaction between magnesium oxide and potassium phosphate is very rapid and needs to be retarded for field application, the second objective of this work is to understand how boric acid, a common admixture, retards the precipitation of K-struvite.

MPC was prepared by mixing hard-burnt magnesia and KH_2PO_4 in equimolar amounts. Cement pastes comprised MPC, low-CaO fly ash used as a filler (fly ash-to-cement weight ratio of 1), and water (water-to-cement weight ratio of 0.56). Additional experiments were performed on cement suspensions (water-to-cement ratios equal to 10 and 100). The boric acid concentration was fixed at 4.17 mmol/L for the study. A panel of techniques was used to investigate the early age hydration of MPC. The evolution of the shear storage modulus, electrical conductivity and heat flow of the cement pastes were monitored with ongoing hydration. In addition, the phase assemblage was characterized after fixed periods of time by X-ray diffraction and thermogravimetry. Complementary experiments on suspensions allowed the evolution of the solution composition to be determined with time.

A multi-stage process was evidenced, depending on the w/c ratio: precipitation of K-struvite could be preceded by the successive formation of newberyite ($MgHPO_4.3H_2O$) and $Mg_2KH(PO_4)_2.15H_2O$. In some cases; $Mg_3(PO_4)_2.22H_2O$ precipitated in addition to K-struvite. Experiments on cement suspensions showed that boric acid did not slow down the initial dissolution of magnesium oxide, but rather retarded the precipitation of the products. The total boron concentration in solution remained constant during the whole hydration process. The $MgB(OH)_4^+$ complex, stabilizing Mg in solution, might be involved in the retardation process. Moreover, in basic medium, boric acid was dissociated into anionic forms ($B(OH)_4^-$, and polyborates at high boron concentration). These negative charges were compensated by an increase in the aqueous concentration of potassium, which in turn tended to favor the formation of $Mg_3(PO_4)_2.22H_2O$ against that of K-struvite.

Originality

Most studies devoted to MPC investigate binders with MgO-to-KH_2PO_4 molar ratio higher than 1. Increasing this ratio is a way to improve the strength development of MPC-based materials, which may be an advantage for rapid repair applications. However, in the field of waste conditioning, the presence of residual magnesium oxide should be avoided since, in the long term, hydration of MgO into $Mg(OH)_2$ may produce deleterious expansion of the material. One originality of this work is thus to focus on the hydration process of a binder with equimolar amounts of MgO and KH_2PO_4.

A robust methodology combining experimental characterizations of the solid and liquid phases with a large panel of techniques is used to investigate the retarding effect of boric acid. Our results contradict the mechanism postulated in the literature according to which dissolution of MgO would be slowed down by the precipitation of a coating layer of lünebergite ($Mg_3B_2(PO_4)_2(OH)_6.6H_2O$) at the surface of the grains or by adsorption of boric acid at the surface of the MgO grains.

Keywords: *magnesium phosphate cement; hydration rate; retardation; mineralogy*

[*] **Corresponding author: hugo.lahalle@cea.fr, Tel +33-4-66397450, Fax +33-4-66397871**

1. Introduction

Magnesium phosphate cements (MPCs) are now well-known for rapid repair works due to their outstanding properties of fast setting and hardening, good volume stability and excellent bonding to old concrete structures (Bensted J., 1994; Yang J., et al, 2000 ; Qiao F., et al, 2010). Moreover, they may also offer prospects for the stabilization / solidification of deleterious wastes which must be conditioned in a stable, monolithic and confined form prior to disposal (Wagh A. S., et al, 1997; Langton C., et al, 2011; Covill A., et al, 2011; Cau Dit Coumes C., et al, 2014).

Magnesium phosphate cement includes magnesium oxide calcined at high temperature (hard-burnt or dead-burnt) and acidic water-soluble phosphate salt, generally diammonium hydrogen phosphate. When an ammonium salt is used, the main product responsible for setting and hardening is struvite, $NH_4MgPO_4.6H_2O$ and byproducts may precipitate under some conditions (Soudée E., 1999). However, the reaction of magnesium oxide with diammonium hydrogen phosphate has the disadvantage of producing ammonia. To avoid the release of noxious gaseous ammonia during the hardening process, ammonium phosphate can be advantageously replaced by potassium dihydrogen phosphate (KH_2PO_4). The main precipitated hydrate is then K-struvite ($MgKPO_4.6H_2O$) (Singh D., et al, 1998).

$$MgO + KH_2PO_4 + 5H_2O \rightarrow MgKPO_4.6H_2O \quad \text{(Eq. 1)}$$

Such a material known as Ceramicrete has been developed in the United States at the Argonne National Laboratory to stabilize hazardous waste (Wagh A. S., 1997). Magnesium phosphate cement prepared from MgO and KH_2PO_4 in the proportions defined by (Eq.1) has a chemical water demand corresponding to a water/cement ratio of 0.51 (cement: MgO + KH_2PO_4). The acidity of KH_2PO_4 solution, near pH 4, increases and stabilizes around 8 after adding MgO (Wagh A. S. et al, 1997). The reaction is highly exothermic. When large volumes of material are prepared, an autocatalytic phenomenon is observed: the heat output increases the temperature of the paste, which further accelerates reaction, so that nearly instantaneous setting can be observed. A retarder such as boric acid (H_3BO_3) or citric acid (typically 2wt% of the binder) must be added to control setting and limit the temperature rise.

Several studies focused on the processes involved in the setting and hardening of magnesium potassium phosphate cement (MPC). For Mg/P ratios comprised between 4 and 12, C. K. Chau (Chau C. K., et al, 2012) *et al.* showed that precipitation of K-struvite ($MgKPO_4.6H_2O$) was preceded by that of $MgHPO_4.7H_2O$, and then of $Mg_2KH(PO_4).15H_2O$. The precipitation sequence depended on pH: $MgHPO_4.7H_2O$ predominated in acidic solution (pH ~ 4), K-struvite formed at pH above 7, and $Mg_2KH(PO_4).15H_2O$ was observed at intermediate pH values ($6 < pH < 8$). By monitoring the electrical conductivity of cement suspensions at lower Mg/P ratio (equal to 1), Le Rouzic (Le Rouzic M., 2013) reported only a two-step mechanism, involving the initial precipitation of newberyite ($5 \leq pH \leq 8$), and the subsequent formation of K-struvite ($6 \leq pH \leq 9$).

Given the high reactivity of MPCs, boric acid is extensively used to delay cement hydration (Hall D. A., et al, 2001 ; Yang J., et al, 2010). The process involved in retardation is however controversial. Several assumptions have been postulated: *(i)* precipitation of a coating layer lünebergite ($Mg_3B_2(PO_4)_2(OH)_6.6H_2O$) at the surface of the cement grains, which would slow down their dissolution (Wagh A. S., 1995 ; Soudée E., 1999), *(ii)* adsorption of $B(OH)_3$ at the surface of the MgO grains, which would also slow down their dissolution (Soudée E., 1999), or *(iii)* stabilization of

aqueous magnesium by formation of a magnesium borate complex in solution (Soudée E. 1999, Hall D. A., et al, 2001).

The objective of this study was thus twofold:

- give new insight into the processes leading to precipitation of K-struvite;
- explain the retardation effect of boric acid.

The focus was placed on a binder comprising equimolar amounts of MgO and KH_2PO_4. Excess of MgO was avoided to discard the risk of deleterious expansion of the material in the long term due to slow hydration of residual MgO into $Mg(OH)_2$. Experiments were performed on cement pastes, but also on diluted suspension for an easier analysis of the solution.

2. Experimental

2.1 Materials

Magnesium phosphate cement comprised equimolar amounts of magnesium oxide MgO (MAGCHEM 10 CR from M.A.F. Magnesite BV, hardburnt grade, d_{10} = 4.8 µm, d_{50} = 18.9 µm, d_{90} = 45.6 µm, specific surface area ~ 0.9 m^2/g) and of potassium dihydrogen phosphate KH_2PO_4 (VWR, purity > 98%, d_{10} = 175 µm, d_{50} = 365 µm, d_{90} = 594 µm).

Cement pastes were prepared with a water-to-cement ratio (w/c) of 0.56 (where c stands for the total mass of MgO and KH_2PO_4). Low-CaO fly ash (composition given in Table 1, d_{10} = 3.0 µm, d_{50} = 24.2 µm, d_{90} = 136.1 µm, specific surface area = 2.2 m^2/g) was used as a filler at a fly ash-to-cement ratio of 1. Fly ash had two beneficial effects: it decreased the temperature rise of the paste during hydration by diluting the cement, and it improved the flowability of the fresh mix. Boric acid was introduced as a retarder in one of the paste specimens. Its dosage (2.54% with respect to the mass of cement – corresponding to 0.73 mol/L in the mixing solution) was slightly below the solubility of boric acid in water at 20°C (0.75 mol/L – Blasdale W.C., et al, 1939).

MgO, KH_2PO_4 and fly ash were mixed in a Turbula blender for 30 minutes. Cement paste volumes of about 100 mL were prepared with an anchor stirrer according to the following protocol: *(i)* start with demineralized water, *(ii)* add premixed powders while stirring at low speed (≈100 rpm), and *(iii)* mix for 2 minutes at high speed (≈200 rpm). When boric acid was used as a retarder, it was previously dissolved in the demineralized water.

Complementary experiments were performed on cement suspensions. The Mg/P ratio was kept to 1. Two water-to-cement ratios (10, and 100) were investigated. In the more diluted systems, boric acid was added at a concentration of 4.17 mmol/L, which corresponded to the same boric acid - to - cement ratio (2.54%) as in the cement paste. Cement suspensions (250 mL) were prepared according to the following protocol: *(i)* dissolve KH_2PO_4, and possibly H_3BO_3, in demineralized water under magnetic stirring (≈200 rpm), *(ii)* add MgO and maintain stirring until the end of the experiment.

Table 1: Chemical composition of fly ash

Raw material	Mass fraction of the sample (%)												
	MgO	Al_2O_3	SiO_2	Fe_2O_3	CaO	TiO_2	MnO	P_2O_5	Cr_2O_3	SrO	Na_2O	K_2O	SO_3
Fly ash	2.15	25.75	50.3	5.92	6.58	1.36	0.08	0.67	0.02	0.27	0.78	1.53	0.80

2.2 Characterization techniques

A panel of techniques was used to investigate the early age hydration of MPC. The evolution of the shear modulus, electrical conductivity and heat flow of the cement pastes were monitored with ongoing hydration. In addition, the phase assemblage was characterized after fixed periods of time by X-ray diffraction and thermogravimetry. Complementary experiments on suspensions allowed the evolution of the solution composition to be determined with time.

2.2.1 Conductimetry and pH monitoring

Hydration of cement suspensions was investigated using a Multicad CDM 210 conductimeter. Experiments were performed in a 250 mL 4hermos-regulated vessel (25°C) under mechanical stirring. The vessel was tightly closed to avoid carbonation and evaporation. The cell was calibrated with a standard KCl solution (12.888 mS/cm at 25°C) before every trial. At constant temperature, the electrical conductivity of the suspension depends on the number and type of ions in solution. Variations in the conductivity thus indicated changes in the chemical composition of the aqueous phase.

Electrical conductivity was also measured on cement pastes. The cell, mainly made of Plexiglass (PMMA), was cylindrically shaped with two annular stainless steel electrodes, an inner radius of 15 mm and a total volume of 70 mL. Temperature was regulated to 25°C by circulation of cooling water in a double envelope. It was connected to the EC channel of an electrochemistry meter (Consort C 861) with a BNC cable. A specific data acquisition software (Consort Dis Data) was used to collect conductivity measurements. The conductivity cell was calibrated using a 12.888 mS/cm standardized KCl solution at 25°C. In paste, a conductivity decrease could be due to a consumption of ions from the pore solution, but also to a decrease in their mobility due to progressive structuring of the material.

The pH of the cement suspensions was measured every 5 minutes with a high-alkalinity electrode (Mettler Toledo Inlab Expert Pt1000 pH 0-14 T 0-100°C) calibrated using standard buffers between 4.1 and 9.2.

2.2.2 Isothermal conduction microcalorimetry

Hydration of cement pastes was followed using a highly sensitive Setaram C80-type microcalorimeter under isothermal conditions at 25.0 ± 0.5°C. Measurements were produced by comparing the heat flow from an experimental chamber containing the hydrating material to that from an inert control chamber with the same total heat capacity.

2.2.3 Rheological measurements

Evolution of the viscoelastic properties of the pastes were followed by dynamic mode rheometry using a strain-driven controlled stress rheometer (AR-G2 TA Instrument, USA). A sinusoidal shear strain γ was applied to the cement paste at constant frequency ω. The resulting stress (τ) was measured by the intermediary of the torque and was also sinusoidal with a δ phase lag with respect to the applied strain.

$$\gamma = \gamma_0 e^{i\omega t} \quad \text{(Eq. 2)}$$

$$\tau = \tau_0 e^{i\omega t + \delta} \quad \text{(Eq. 3)}$$

Within the linear viscoelasticity range, the ratio between the stress and the shear strain is equal to the complex shear modulus (G*) and is defined by:

$$G^* = G' + iG'' \quad \text{(Eq. 4)}$$

with G' the shear storage modulus, and G'' the shear loss modulus.

For the investigated samples, the critical strain (γ_c) was found to be close to 0.05%. In order to stay in the linear viscoelasticity domain of the materials, and thus to avoid destructive measurements, experiments were performed using a 10^{-4} shear strain and a 1 rad/s frequency. A specific vane geometry (stainless steel) was used to perform all the experiments. This geometry was selected for two reasons:

- the same tool could be used to perform measurements in the dynamic mode, but also to mix the sample to get a better homogeneity just before the rheometric characterization,
- it was much less sensitive to segregation than the classic parallel plate geometry.

The vane geometry was calibrated with standard oil (S600, 2.089 Pa.s, PSL), as well as with a non-Newtonian fluid (water + 0.5% Xanthan).

2.2.4 Vicat setting time

The Vicat setting time was measured according to standard European procedure EN 196-3. The needle was on a 300 g moveable rod and had a diameter of 1 mm ± 0.05 mm. A sample of fresh cement paste was cast in a frustum 40 mm in height. Initial setting time was considered as the time when the needle penetration was 39 mm ± 0.5 mm. The final setting time corresponded to less than 0.5 mm penetration.

2.2.5 Mineralogical characterizations

Cement hydration was stopped after fixed periods of time. The paste samples were crushed, immersed into isopropanol and dried in a controlled humidity chamber (with 20% relative humidity at 22 ± 2°C). Cement suspensions were filtered on a Buchner funnel. The solid phases were rinsed with isopropanol, and dried at 22 ± 2°C and 20% relative humidity. Crystallized phases were identified by X-ray diffraction with the Bragg Brentano geometry (PanAlytical X'pert Pro, copper anode, $\lambda_{K\alpha 1}$=1.54056 Å, 40 mA and 40 kV, scanning from 2θ = 5° to 60° in 0.017° steps, 50 s measurement time per step) on pastes ground by hand to a particle size less than 100 µm. Thermogravimetric analyses were carried out under N_2 atmosphere on 50 ± 2 mg of sample using a TGA/DSC Netzsch STA 409 PC instrument at 10°C / min up to 1000°C.

2.2.6 Analysis of solutions

The composition of the aqueous phase of cement suspensions was determined after increasing periods of hydration. 1mL aliquots of the solution were sampled using a syringe, filtered at 0.45 µm and diluted before analysis by ICP-AES. The analytical error was ± 5%.

3. Results and discussion

3.1 Hydration of MPC in the absence of boric acid

3.1.1 Cement paste

Figure 1 shows the evolution with time of the electrical conductivity, heat flow and shear storage modulus of a cement paste comprising MgO, KH_2PO_4, fly ash and water.

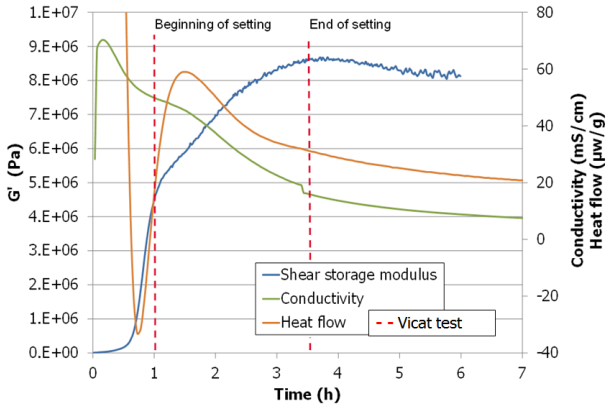

Figure 1 : Evolution of the electrical conductivity, heat flow and shear storage modulus of a MPC paste during hydration (MgO + KH_2PO_4 + fly ash, w/c = 0.56).

The shear storage modulus began to increase after 30 minutes, indicating a precipitation of hydrates which was thus responsible for the first drop in the electrical conductivity. The modulus growth was very rapid from 30 minutes to 1 hour (which also corresponded to the beginning of setting determined using the Vicat needle), and then slower from 1 h to 3 h 30 min (end of setting). The decrease observed after 4 h might be an artefact due to difficult measurements in the hardened material.

After a rapid increase resulting from a start of dissolution of the anhydrous cement phases, the electrical conductivity decreased in two stages. This decrease could result from two factors: *(i)* a variation in the composition of the interstitial solution resulting from the precipitation of hydrates, as evidenced by the simultaneous increase in the shear storage modulus, and also, especially for the second drop, *(ii)* a decrease in the mobility of the ionic species due to the progressive depercolation of the porous network caused by the precipitation of large amounts of hydrates.

During the first 30 minutes after mixing, the calorimetric signal was biased by extra undesirable heat caused by frictions when the calorimetric cell was introduced in the calorimetric chamber, and thus could not be interpreted. Then, from 30 min to 50 min, an endothermic process predominated.

This indicated a strong dissolution of KH_2PO_4 ($KH_2PO_4 \rightarrow K^+ + H_2PO_4^-$, ΔH_r = 26.2 kJ/mol). After 50 min, hydration became exothermic. The heat production could result from several reactions such as dissolution of MgO ($MgO + H_2O \rightarrow Mg^{2+} + 2\ OH^-$, ΔH_r = -39.5 kJ/mol) and precipitation of K-struvite ($Mg^{2+} + K^+ + H_2PO_4^- + 5\ H_2O \rightarrow MgKPO_4.6H_2O$; ΔH_r = -283.9 kJ/mol). The heat flow reached its maximum after 1 h 45 min, and then decreased less and less rapidly.

To correlate these evolutions with mineralogical changes, hydration was stopped at characteristic times of the electrical conductivity curve (15 min, 30 min, 1 h, 1 h 40 min, 3 h 45 min, 5 h 30 min, 27 h, 7 d and 26 d), and the phase assemblage was characterized using X-ray diffraction (Figure 3) and thermogravimetry (Figure 4).

Quartz and mullite, two non-reactive phases from fly ash, were detected whatever the characterization time. Potassium dihydrogen phosphate rapidly dissolved during the first hours of hydration: only traces were observed after 5 h 30 min, and this mineral was not detected anymore after 24 h. Magnesium oxide dissolved more slowly, and was still present in small amounts after 26 d. K-struvite was detected from the first characterization time, as traces up to 30 min, and in much higher amount from 1 h, once hydration accelerated. From 3 h 45 min, other minerals were detected, possibly $MgHPO_4.7H_2O$, $AlPO_4.xH_2O$, $Mg_3Si_2O_5(OH)_4$ (lizardite), $Ca_6Si_2O_7(OH)_6$ (jaffeite). However, given the weak intensity and overlapping of their diffraction peaks, they could not be identified with certainty. The precipitation of aluminate and silicate hydrates would indicate a partial reaction of fly ash. Newberyite and $Mg_2KH(PO_4)_2(H_2O)_{15}$, mentioned as transient products in the literature, could not be evidenced by X-ray diffraction. However, the thermograms recorded from the first characterization time (15 min) showed a weight loss at about 80°C. It could not be attributed to K-struvite, the sole crystallized hydrate detected at an early age, since this mineral begins to dehydrate at 136 °C (Le Rouzic M., et al, 2014). It was thus concluded from thermogravimetry analysis that an amorphous or poorly crystallized hydrate formed in the early stages of hydration. Its precipitation could explain why the increase in the shear storage modulus and the decrease in the electrical conductivity started as soon as 30 min, despite the small amount of K-struvite formed at that time.

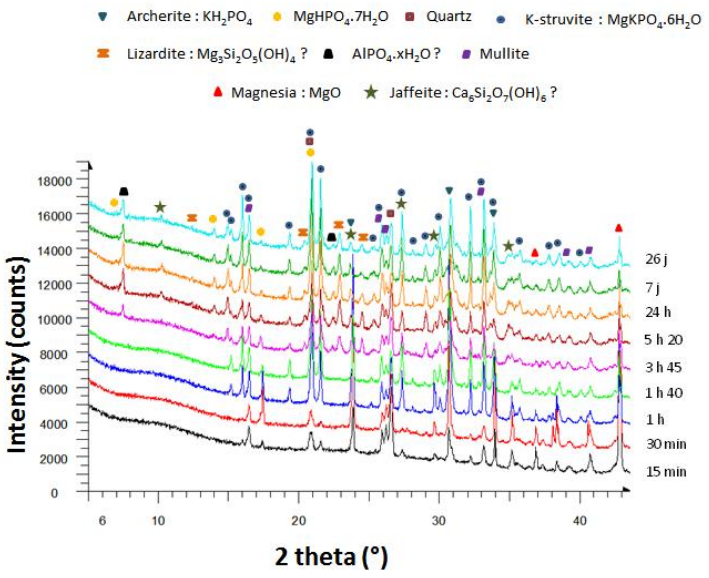

Figure 2: X-ray diffraction patterns of MPC paste aged from 15 min to 26 d ($MgO + KH_2PO_4$ + fly ash, w/c = 0.56)

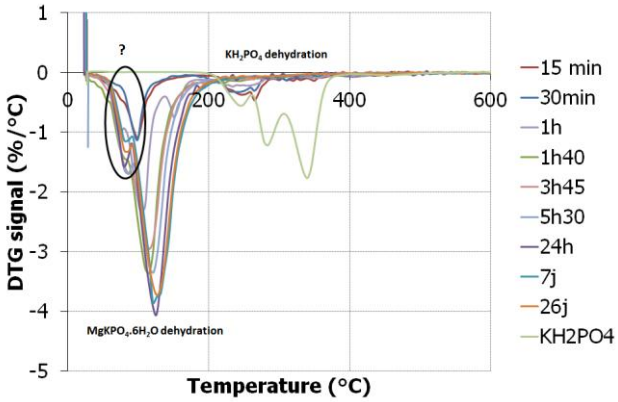

Figure 3: Thermograms of MPC paste aged from 15 min to 26 d (MgO + KH_2PO_4 + fly ash, w/c = 0.56)

3.1.2 Diluted suspension (w/c =10)

Since hydration of MPC was very rapid as a paste, it was slowed down by increasing the w/c ratio to 10. Figure 4 shows the evolution of the pH and electrical conductivity of the cement suspension with ongoing hydration.

The electrical conductivity increased rapidly during the first hour, reached a maximum, and then decreased in two steps. The pH increased from 4.3 to 10.2 over the duration of the experiment, but in a non-monotonous way: three transient drops occurred at 1 h, 1 h 30 min and 3 h 30 min. The mineralogical evolution of the solid fraction was characterized by X-ray diffraction (Figure 5).

- At 30 min, significant amounts of newberyite $MgHPO_4.3H_2O$ were detected, as well as traces of the more hydrated $MgHPO_4.7H_2O$ phase (phosphorroesslerite). It should be noted that this phase is very unstable and easily transforms into newberyite (Khiel S.J., et al, 1933). Thus, it cannot be excluded that $MgHPO_4.7H_2O$ precipitated instead of newberyite in the cement paste, but was later converted into newberyite when the paste samples were dried prior to mineralogical characterization.
- At 1 h, newberyite was converted into $Mg_2KH(PO_4)_2.15H_2O$;
- At 1 h 30 min, $Mg_2KH(PO_4)_2.15H_2O$ was destabilized in favor of K-struvite whereas newberyite was detected again;
- At 2 h, newberyite was almost fully depleted, and $Mg_2KH(PO_4)_2.15H_2O$ precipitated again;
- At 3 h 30 min, only traces of $Mg_2KH(PO_4)_2.15H_2O$ were detected and the amount of K-struvite increased sharply;
- At 7 h, hydration was complete; MgO was fully consumed, and K-struvite was the sole crystallized hydrate detected by X-ray diffraction.

Balance equation (Eq. 5), describing the formation of newberyite from MgO and $H_2PO_4^-$, consumed some protons and could thus explain the initial pH increase.

$$MgO + H_2PO_4^- + H^+ + 2\,H_2O \rightarrow MgHPO_4.3H_2O \qquad \text{(Eq. 5)}$$

By contrast, conversion of newberyite into $Mg_2KH(PO_4)_2.15H_2O$ (Eq. 6) released some protons, resulting in the first pH drop at 1 h.

$$2\ MgHPO_4.3H_2O + K^+ + 9\ H_2O \rightarrow Mg_2KH(PO_4)_2.15H_2O + H^+ \quad \text{(Eq.6)}$$

In the same way, conversion of $Mg_2KH(PO_4)_2.15H_2O$ into K-struvite (Eq. 7) also yielded some protons, which could explain the two other pH drops at1 h 30 min and 3 h 30 min.

$$Mg_2KH(PO_4)_2.15H_2O + K^+ \rightarrow 2\ MgKPO_4.6H_2O + 3\ H_2O + H^+ \quad \text{(Eq. 7)}$$

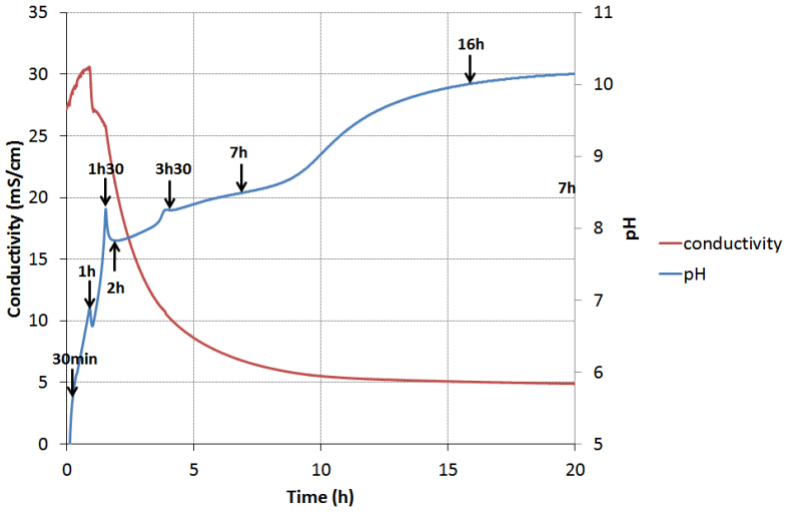

Figure 4: Evolution of pH and electrical conductivity of the MPC suspension with ongoing hydration ($MgO + KH_2PO_4 + H_2O$, w/c = 10)

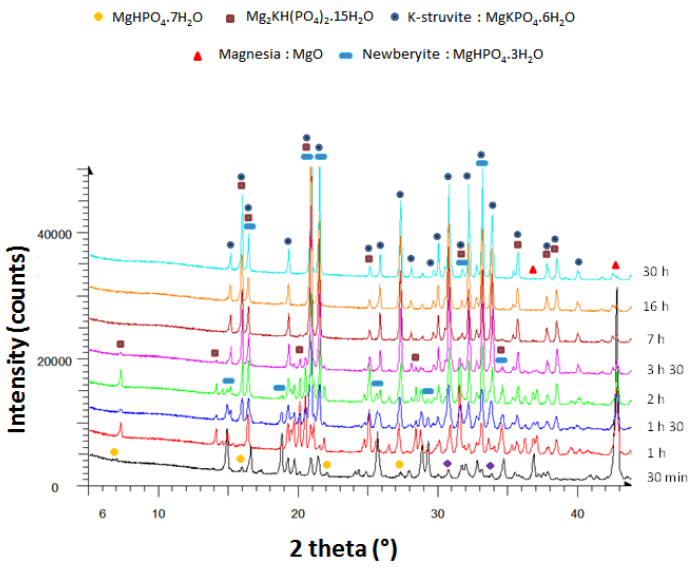

Figure 5: X-ray diffraction patterns of the solid fraction of MPC suspension from 30 min to 30 h ($MgO + KH_2PO_4 + H_2O$; w/c =10)

Therefore, hydration of MPC involved three steps: precipitation of newberyite, conversion into $Mg_2KH\ (PO_4)_2.15H_2O$, which subsequently formed K-struvite. Since dissolution of MgO was not instantaneous, newberyite still precipitated while $Mg_2KH(PO_4)_2(H_2O)_{15}$ was transformed into K-

struvite. The pH at the end of the reaction was unexpectedly high. Formation of K-struvite according to balance equation (Eq. 1) should not lead to any pH change. The equilibrium pH of K-struvite is reported to be close to 7-8 (Wagh A. S., et al, 1997). The measured pH of 10.2 may indicate the presence of other minerals (e.g. $Mg_3(PO_4)_2.xH_2O$), present in too small amount to be detected by X-ray diffraction, but which would contribute to control the pH.

Thermogravimetry analysis (Figure 6) confirmed the precipitation of transient products, in addition to K-struvite. Three thermal events were indeed observed for temperatures close to 80°C, 130°C and 150°C. According to literature (Le Rouzic M., et al, 2014), the weight losses at 130°C and 150°C could be attributed to dehydration of K-struvite ($MgKPO_4.6H_2O \rightarrow MgKPO_4 + 6\ H_2O$) and newberyite ($MgHPO_4.3H_2O \rightarrow MgHPO_4 + 3$ H2O) respectively. The weight loss at 80°C likely corresponded to dehydration of $Mg_2KH(PO_4)_2.15H_2O$. It was maximal at 1 h, time at which the X-ray diffraction peaks of $Mg_2KH(PO_4)_2.15H_2O$ showed the strongest intenisty.The total weight loss measured at the end of the experiment (39.8%) was in good agreement with that calculated according to (Eq. 1) assuming full conversion of MgO into K-struvite (40.1%).

It should be pointed out that, at an early age, the cement paste also exhibited a weight loss at a temperature close to 80°C. Although $Mg_2KH(PO_4)_2.15H_2O$ was not detected by X-ray diffraction in this material, assuming its precipitation as a poorly crystallized product could not be excluded.

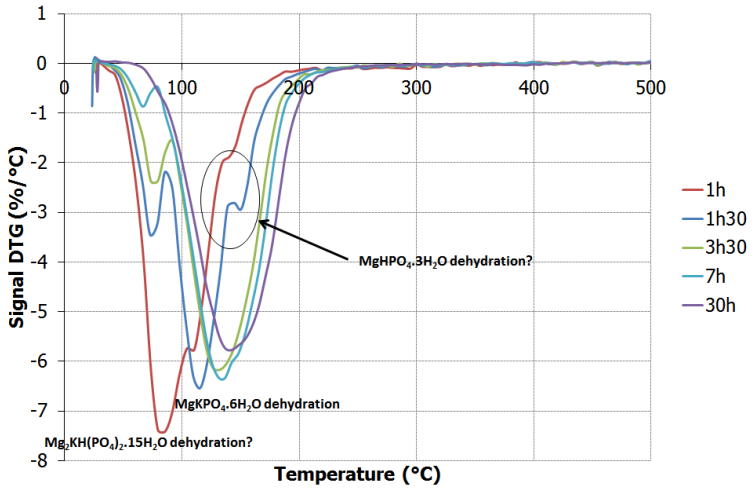

Figure 6: Thermograms of MPC suspension from 1 h to 30 h ($MgO + KH_2PO_4 + H_2O$, w/c =10)

3.2 Influence of boric acid on MPC hydration

3.2.1 Cement pastes

Figure 7 shows the influence of H_3BO_3 on the hydration rate of a MPC paste. The electrical conductivity of the cement paste exhibited the same evolution (rapid increase, followed by a two-stage decrease) as the reference free from boric acid, but on a much longer period of time. In agreement with previously reported results, boric acid strongly retarded cement hydration.

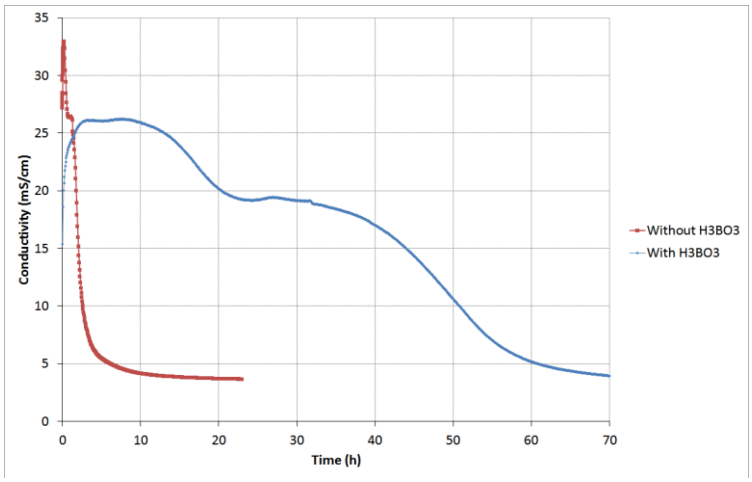

Figure 7: Influence of boric acid (2.54% with respect to cement) on the electrical conductivity of a MPC paste (w/c = 0.56).

3.2.1 Diluted suspensions (w/c =100)

As previously, complementary investigations were performed on cement suspensions in order to better characterize the different stages of hydration. The w/c ratio was raised to 100, which allowed the number of aliquots sampled for ICP-AES analysis to be increased.

Figure 8 compares the electrical conductivity and pH of suspensions with (4.17 mmol/L) and without boric acid. During the first hour, both systems exhibited very similar evolutions. Retardation in the system containing boric acid was noticeable afterwards, when the pH exceeded 7. The non-monotonous variations of conductivity and pH with time showed again a multi-stage process.

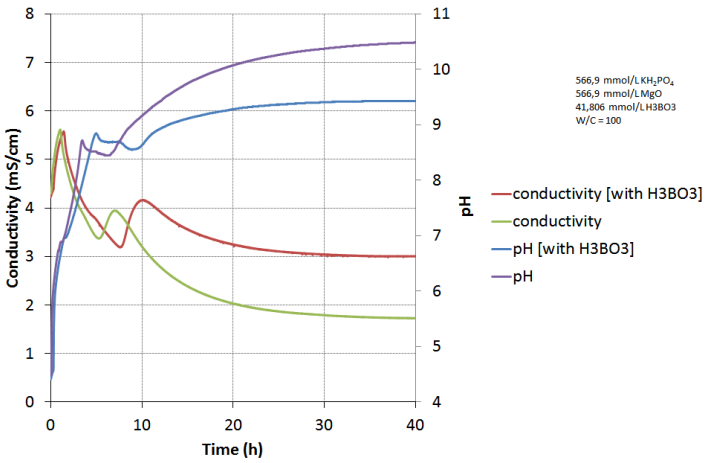

Figure 8: pH and electrical conductivity evolution over time for two diluted MPC suspensions, one system including MgO, KH_2PO_4 and H_2O, the other MgO, KH_2PO_4, H_3BO_3 and H_2O (w/c =100).

The phase assemblage evolution of both systems was characterized by X-ray diffraction (Figure 9, Figure 10) and thermogravimetry (Figure 11, Figure 12). Regardless the boric acid concentration, $Mg_2KH(PO_4)_2.15H_2O$ precipitated first and was subsequently converted into K-struvite and $Mg_3(PO_4).22H_2O$. It should be pointed out that the suspension with boric acid did not contain any crystallized boron-containing mineral, such as the lünebergite phase ($Mg_3B_2(PO_4)_2(OH)_6.6H_2O$) mentioned in the literature. $Mg_3(PO_4).22H_2O$ seemed to dehydrate below 100°C, in the same range of temperatures as $Mg_2KH(PO_4)_2.15H_2O$. The distinction between these two phases was thus difficult by

thermogravimetry analysis. The solid fraction of the suspension with boric acid exhibited a higher total weight loss after 30 h than that of the reference free from boric acid. This could be explained by higher amounts of $Mg_3(PO_4).22H_2O$, a phase containing more bound water than K-struvite.

Increasing the w/c ratio from 10 (section 3.1.2) to 100 (this section) influenced the first stage of hydration: newberyite did not precipitate anymore. It also promoted the formation of $Mg_3(PO_4)_2.22H_2O$ at later age. This phase was clearly identified by X-ray diffraction in the most diluted suspension, whereas its presence was only postulated due to the high pH in the less diluted suspension.

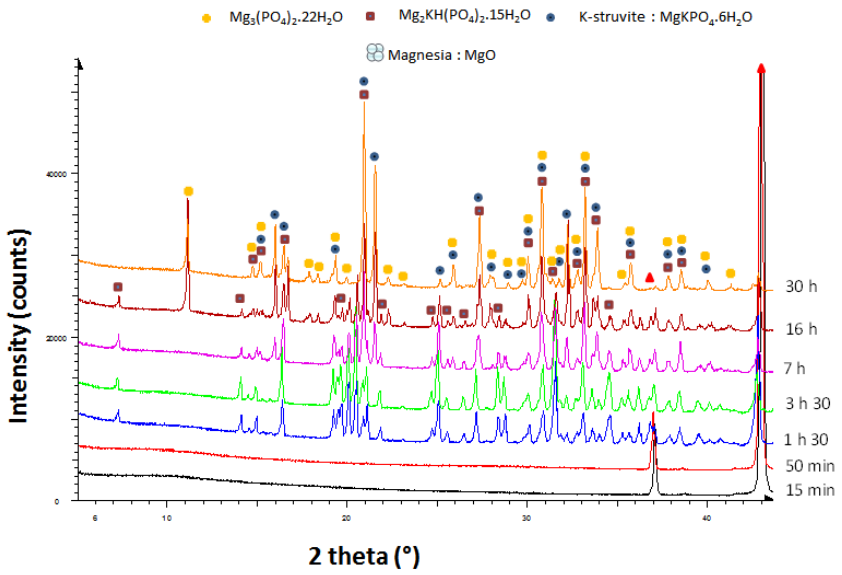

Figure 9: X-ray diffraction patterns of MPC suspension from 15 min to 30 h ($MgO + KH_2PO_4 + H_2O$, w/c =100)

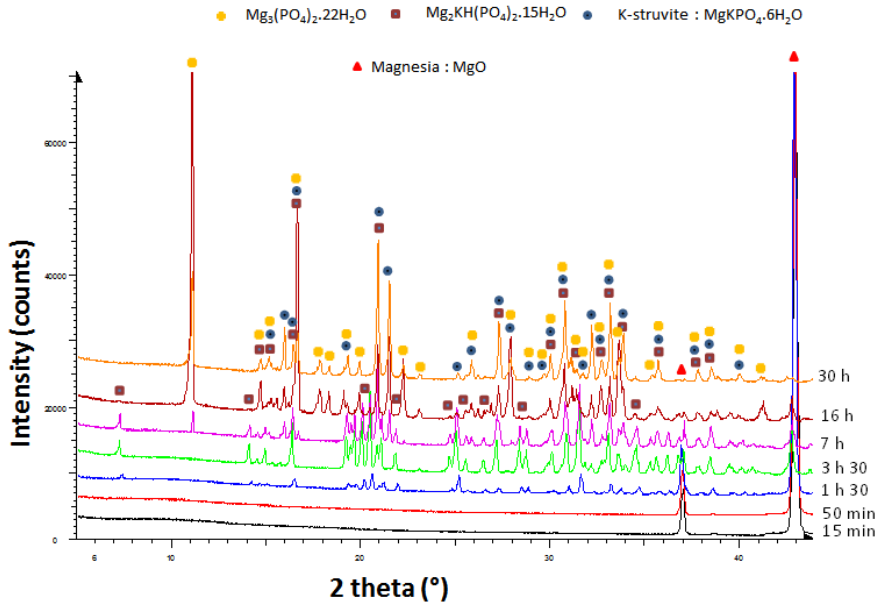

Figure 10: X-ray diffraction patterns of MPC suspension with boric acid from 15 min to 30 h ($MgO + KH_2PO_4 + H_3BO_3 + H_2O$, w/c =100)

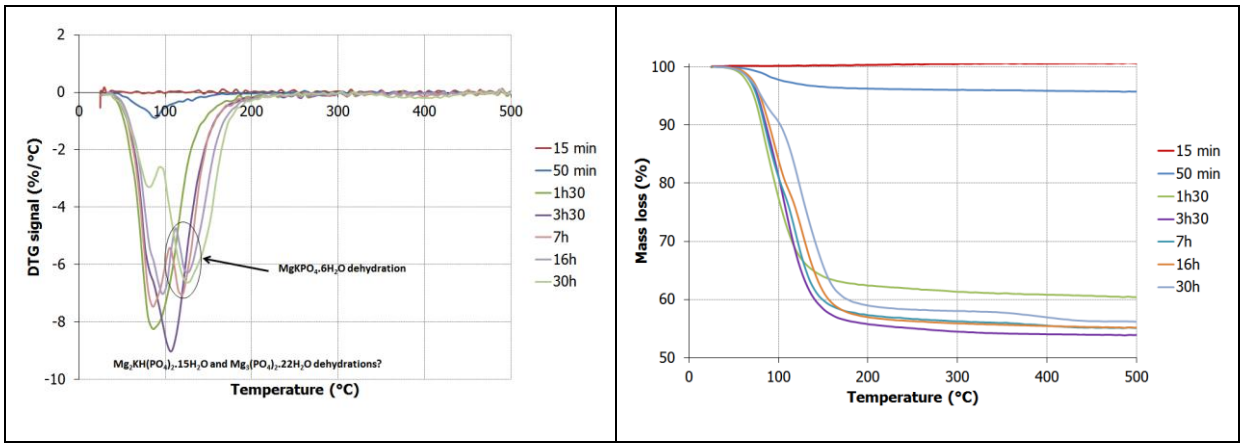

Figure 11: Thermograms of MPC suspension from 15 min to 30 h (MgO + KH_2PO_4 + H_2O, w/c =100)

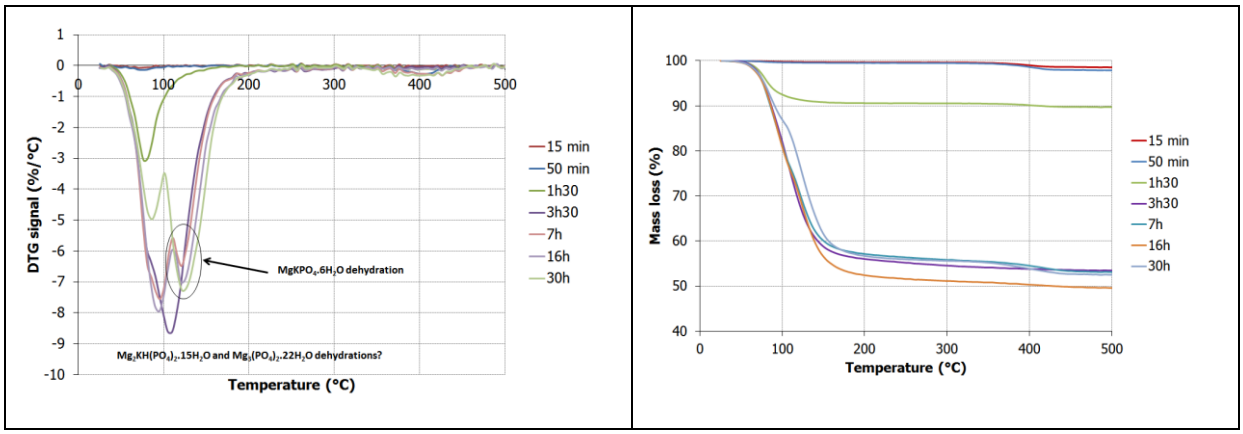

Figure 12: Thermograms of MPC suspension with boric acid from 15 min to 30 h (MgO + KH_2PO_4 + H_3BO_3 + H_2O, w/c =100)

Solid phase characterization of the cement suspensions was supplemented by analyses of the liquid phase by ICP-AES. Figure 13 shows the evolution over time of the B, Mg, K and P concentrations in solution for the system with boric acid ($[B]_{tot}$ = 4.17 mmol/L).

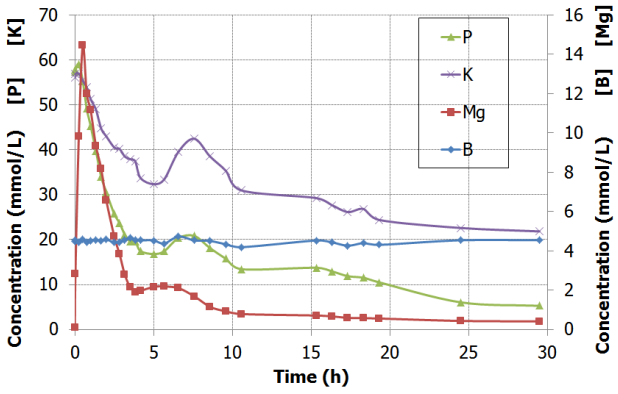

Figure 13: Composition of the aqueous fraction of MPC suspension with ongoing hydration (MgO + KH_2PO_4 + H_3BO_3 + H_2O, w/c =100)

The boron concentration remained constant during the whole experiment, equal to its initial value. Mechanisms assuming precipitation of boron or adsorption onto MgO to explain its retarding effect could thus be discarded.

From 0 to 15 minutes, the K and P concentrations remained constant, equal to their initial values (taking into account the measurement uncertainties), whereas the Mg concentration increased sharply. This first stage thus corresponded to dissolution of MgO. Then, from 15 min to about 5 h, a simultaneous decrease in the concentrations of Mg, P and K was observed. The ratio between the slopes of the regression lines fitting the K and P concentration curves was close to 0.5 (calculated value of 0.53), which was consistent with the precipitation of $Mg_2KH(PO_4)_2.15H_2O$. From 5 h to 7 h, the Mg, K and P concentrations exhibited a transient increase, indicating the dissolution of $Mg_2KH(PO_4)_2.15H_2O$ which released Mg^{2+}, K^+ and HPO_4^{2-} ions in solution. After 7 h, the concentrations decreased again. The slope ratio between the regression lines fitting the K and P concentration curves between 10 and 30 h was slightly lower than unity (calculated value of 0.92), showing that a potassium-free phase could precipitate in addition to $MgKPO_4.6H_2O$. This phase was identified as $Mg_3(PO_4)_2.22H_2O$ by X-ray diffraction.

Figure 14 compares the evolution of the Mg, K and P concentrations in the two systems with and without boric acid.

The initial dissolution of MgO was not influenced by the presence of boric acid (Figure 16-a): during the first 30 minutes, both systems exhibited the same Mg concentration in solution. Thus, retardation of MPC by boric acid could not be explained by a slower initial dissolution of the reactant. However, differences were noticed from 1 to 2 h. The decrease in the Mg concentration was slower in the presence of boric acid. This decrease resulted from a competition between MgO dissolution (which released Mg^{2+} ions in solution) and precipitation of $Mg_2KH(PO_4)_2.15H_2O$ (which consumed Mg^{2+} ions from the solution). Since dissolution of MgO did not seem to depend on the boric acid concentration, it was rather the precipitation of $Mg_2KH(PO_4)_2.15H_2O$ which was affected. Thermograms at 50 min and 1 h 30 min (Figures 11 and 12) confirmed that the amount of precipitated hydrate was much smaller in the sample with boric acid than in the reference. Boric acid might thus retard the formation of this product, either directly or indirectly by stabilizing Mg in solution as a $MgB(OH)_4^+$ complex as postulated by Soudée (Soudée E., 1999). During this period, the aqueous concentrations of phosphate and potassium were also higher in the system containing boric acid than in the reference.

Destabilization of $Mg_2KH(PO_4)_2.15H_2O$, releasing Mg^{2+}, HPO_4^{2-} and K^+ in solution, was not significantly delayed by boric acid. However, the second decrease in the Mg^{2+}, K^+ and HPO_4^{2-} concentrations due to precipitation of K-struvite and $Mg_3(PO_4)_2.22H_2O$ seemed to be slightly slower. Thus, boric acid seemed to slow down the formation of products rather than the dissolution of MgO.

After 20 h, the residual aqueous concentration of potassium was significantly higher in the system with boric acid. This could be simply explained by electrical balance. At pH ~10, boric acid was partly ionized, mainly as $B(OH)_4^-$. These additional negative charges needed to be compensated by cations. A thermodynamic calculation using the Chess software (Van der Lee J., 1998) and its database completed with borate and polyborate species (Champenois J. B., et al, 2015) showed that, for a pH of 9.6 and total P, Mg and B concentrations of 9.04 mmol/L, 0.43 mmol/L and 4.2 mmol/L respectively (values measured experimentally at 24 h), a total K concentration of 21.1 mmol/L was needed to keep electroneutrality. This calculated value was in fairly good agreement with that measured experimentally (21.6 mmol/L). The increased solubility of potassium in the presence of

boric acid could explain why precipitation of $Mg_3(PO_4).22H_2O$ seemed to be favored against that of $MgKPO_4.6H_2O$ under such conditions.

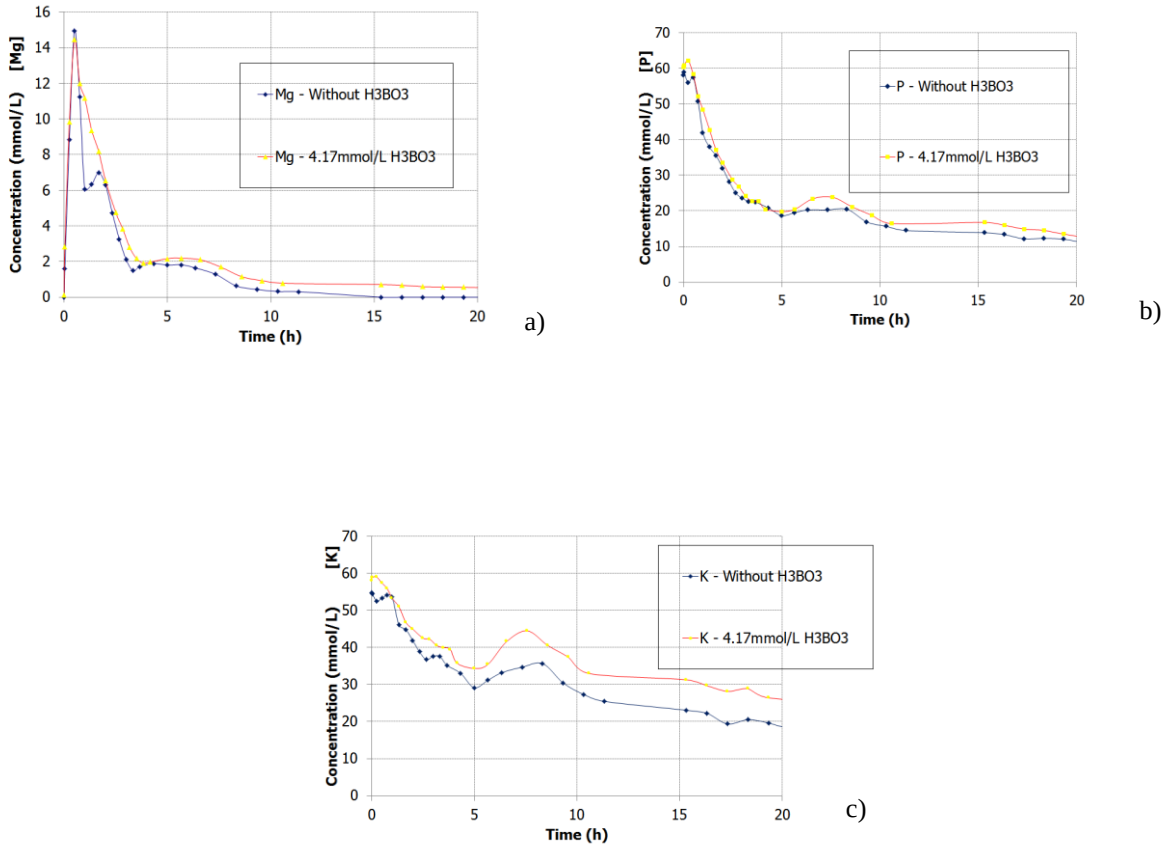

Figure 14: Influence of boric acid on the evolution of Mg, P and K concentrations in the aqueous phase of MPC suspensions (w/c = 100)

4. Conclusion

This work, focused on the hydration of magnesium phosphate cement and on its retardation by boric acid, led to the following conclusions.

1. Hydration of MPC is a multi-step process. The sequence of phase precipitation depends on the w/c ratio. At w/c = 0.56 (cement paste), precipitation of K-struvite is preceded by that of an amorphous or poorly crystallized product dehydrating in the same range of temperatures as $Mg_2KH(PO_4)_2.15H_2O$. At w/c = 10 (cement suspension), newberyite, and/or its more hydrated analogous $MgHPO_4.7H_2O$, first precipitate. These phases are then destabilized to form $Mg_2KH(PO_4)_2.15H_2O$ which is finally converted into K-struvite. At w/c = 100 (diluted cement suspension), $Mg_2KH(PO_4)_2.15H_2O$ forms initially, and then yields K-struvite and $Mg_3(PO_4)_2.22H_2O$.

2. Low-CaO fly ash used as a filler in MPC pastes, is partly reactive, leading to the precipitation of aluminate and silicate hydrates.

3. Boric acid retards MPC hydration. Under the conditions of the study (diluted cement suspebsion) boron is not precipitated within the cement hydrates, nor adsorbed at the surface of the MgO grains, but rather remains in solution. Boric acid does not slow down the initial dissolution of MgO, but seems to retard the precipitation of the products. The $MgB(OH)_4^+$ complex, stabilizing Mg in solution, might be involved in the retardation process. Moreover, in basic medium, boric acid is dissociated into anionic forms ($B(OH)_4^-$, and polyborates at high boron concentration). These negative charges are compensated by an increase in the aqueous concentration of potassium, which in turn tends to favor the formation of $Mg_3(PO_4)_2.22H_2O$ against that of K-struvite.

Future work will be focused on the influence of the w/c ratio on the mechanism by which boric acid retards MPC hydration.

Acknowledgements

This work was supported by the interdisciplinary NEEDS project funded by ANDRA, CNRS, EDF, AREVA, CEA and IRSN.

References

- Bensted J., 1994. Rapid setting magnesium phosphate cement for quick repair of concrete pavements - characterization and durability aspects - Discussion. *Cement and Concrete Research* 24**,** 595-596.

- Blasdale W. C., et al, 1939. The solubility curves of boric acid and the borates of sodium.. *Journal of the American Chemical Society*, 61**,** 917-920.

- Cau Dit Coumes C., et al, 2014. Selection of a mineral binder with potentialities for stabilization/solidification of aluminum metal. *Journal of Nuclear Materials,* 453**,** 31-40.

- Champenois J. B., et al, 2015. Influence of sodium borate on the early age hydration of calcium sulfoaluminate cement. *Cement Concrete research,* 70**,** 83-93.

- Chau C. K., et al, 2012. Potentiometric Study of the Formation of Magnesium Potassium Phosphate Hexahydrate. *Journal of Materials in Civil Engineering*, 24, 586-591.

- Covill A., et al, 2011. Development of magnesium phosphate cements for encapsulation of radioactive waste. *Advanced in Applied Ceramics*, 110, 151-156.

- Hall D. A., et al, 2001. The effect of retarders on the microstructure and mechanical properties of magnesia–phosphate cement mortar. *Cement and Concrete Research*, 31, 455-465.

- Kiehl S. J., et al, 1933. The dissociation pressures of magnesium ammonium phosphate hexahydrate and sole relared substances, VII. *Journal of the American Chemistry Society*, 55, 605-618.

- Stefanko D. B., et al, 2010. Magnesium monopotassium phosphate grout for P-reactor vessel in-situ decommissioning, *Savannah River National Laboratory Report, SRNL-STI-2010-00333 Revision 0*, 60 p

- Qiao F., et al, 2010. Property evaluation of magnesium phosphate cement mortar as patch repair material. *Construction and Building Materials*, 24, 695-700.

- Le Rouzic M., et al, 2014. Formation of k-struvite in magnesium phosphate cement. *NUWCEM, 2nd International Symposium on Cement-based Materials for Nuclear Wastes*, Avignon 3-6 June 2014. Avignon : Palais des papes. *Theses*

- Singh D., et al, 1998. Phosphate ceramic process for macroencapsulation and stabilization of low-level debris wastes. *Waste Management*, 18, 135-143.

- Soudée E., 1999. *Liants phospho-magnésiens : mécanisme de prise et durabilité*. French thesis (PhD). INSA de Lyon, France.

- Van der Lee J., 1998. *Thermodynamic and mathematical cocepts of CHESS*. Technical Report LHM/RD/98/39, 99p.

- Wagh A. S., et al, 1995. Stabilization of Hazardous ash waste with newberyite-rich chemically bonded magnesium phosphate ceramic. *Journal of Materials Research*, 29, 04, 35p.

- Wagh A. S., et al, 1997. Stabilization of contaminated soil and wastewater with chemically bonded phosphate ceramics, *Proc. Waste Management 1997 (WM'97)*, Tuscon, USA.

- Wagh A. S., et al, 1997. Ceramicrete stabilization of low-level mixed wastes, a complete story, *Proc. 18th Annual DOE Low-Level Radioactive Waste Management Conference*, Salt Lake City, USA.

- Yang J., et al, 2000. Characteristics and durability test of magnesium phosphate cement-based material for rapid repair of concrete. *Materials and Structures*, 33, 229-234.

- Yang J., et al, 2010. Effect of borax on hydration and hardening properties of magnesium and potassium phosphate cement pastes. *Journal of Wuhan University of Technology-Mater. Sci. Ed*, 25, 613-618.